SMART SENSORS FOR MEASURING FLUID FLOW USING A VENTURI CHANNEL

Cornelius E. Agu and Bernt Lie[1]
Faculty of Technology, Telemark University College
Norway

ABSTRACT

In certain applications, the use of a direct flow meter to measure flow rates could be very expensive due to size, and may give inaccurate results due to adverse operating conditions. One alternative is to use an open channel flow measurement technique. The use of a hydraulic structure such as Venturi flume with one point level measurement is robust enough to estimate the flow rate. However, flow rates estimated by using the flow-depth relationship established in the channel are only accurate in steady state conditions. For conditions where the free surface flow is influenced by waves such as flows in oil platform, river flow in hydropower, fluidized powder transport, etc., steady state free surface level is barely reached within the required control time. This study presents a smart system for continuous measurement of fluid flow rate in a Venturi channel, which is required for control purposes. The method developed and presented here is based on merging the level measurements with the one-dimensional Saint Venant equation through a Kalman filter to provide real-time estimation of flow rate for both Newtonian and non-Newtonian fluids.
Keywords: Smart Sensor, Venturi channel, Saint-Venant Equation, Real-time estimation, Kalman filter.

[1] Corresponding author, E-mail: bernt.lie@hit.no

NOMENCLATURE

A Cross sectional area [m^2]
$\bar{A}$ Average cross sectional area [m^2]
f Coefficient
b Channel width [m]
C Observation matrix
E Innovation covariance matrix
e Error
Fr Froude number
g Gravitational acceleration [m/s^2]
h Free surface level [m]
K Flow behaviour index [$Pa.s^n$]
K Kalman gain
N Spatial grid size
N_r Ensemble size
n Fluid consistency index
P_{wet} Wetted perimeter [m]
Q Flow rate [m^3/s]
R_h Hydraulic radius [m]
S Slope
u Model input
V Average velocity [m/s]
V Measurement noise covariance matrix
v Measurement noise vector
w Process noise vector
W Process noise covariance matrix
X Estimated state covariance matrix
x Distance
x State vector
$\hat{x}$ Estimated state vector
$\bar{x}$ Mean value
y Measurement signal vector
$\hat{y}$ Estimated measurement signal vector
Z Cross covariance matrix
β Momentum correction coefficient
Σ Error matrix
$\boldsymbol{\rho}$ Density [kg/m^3]
θ Inclination of the channel bottom [degree]
θ Model parameter vector
$\hat{\theta}$ Estimated model parameter
$\boldsymbol{\tau_y}$ Yield shear stress [Pa]

Subscripts

x State
0 Bottom origin; initial condition
c Critical
i Index in space
in Inlet
out Outlet
θ Parameter

Superscripts

0 Initial condition
a Assimilated
f Forecast
j Index in size
k Index in time
T Transpose

INTRODUCTION

Fluid flow in an open channel has wide industrial applicability. It is used in transportation of slurries, water supply for irrigation and river flow [1]. Due to severe operating conditions, use of common flow meters may be considered very expensive or unsafe to measure the flow rate of slurries (non-Newtonian fluids). One common and simple method is to use an open channel hydraulic structure such as a "weir" (Notch) or a "control flume" which introduces a restriction in the flow direction that results in flow variations (that is, changes in approach velocity and level) along the channel [2]. Flumes are commonly used in the industry. The flow-depth relationship established in control flumes is only applicable in steady state [3]. For conditions such as flows in oil platform, river flow in hydropower, fluidized powder transport, etc., where the free surface flow is influenced by waves, a steady state free surface level is barely reached within the required control time. In this situation, estimating any flow rate in the channel will require a real-time estimation technique.

A real-time estimation technique requires knowledge about a model which accurately describes the system, and that the system must be observable. For an observable system, it follows

that from an output of the system the behavior of the entire system can be determined. For simplicity, one-dimensional Saint Venant equation is commonly used to model an open channel flow [4]. Several techniques have been used to incorporate a measurement from the physical system into the Saint Venant equation for state estimation in an open channel flow. Most of these methods are based on Kalman filter algorithms applied to linear models [5, 6, 7]. The use of the standard Kalman filter will require linearizing the Saint Venant model, and this may mean not capturing some important detail of the system, especially when there is rapid variation of the system boundary conditions [7]. In [8], the Extended Kalman filter was applied to estimate uncertain parameters in two-dimensional shallow water models. The Extended Kalman filter (EKF) involves computation of the Jacobian at every time step which increases the computation burden [9]. The Ensemble Kalman filter (EnKF) is an alternative to the Extended Kalman filter, and is based on Monte Carlo simulation of the nonlinear system [9]. The Ensemble Kalman filter was originally developed for data assimilations in weather prediction and other areas involving large use of data [10]. In [9], the author used EnKF to incorporate Lagrangian measurements into a two-dimensional shallow water model with poorly known boundary conditions.

The main purpose of this study is to investigate a smart system for continuous measurement of fluid flow rate in an open channel. In the present work, we apply the Ensemble Kalman filter scheme to estimate the real-time flow rate of fluid in a Venturi channel. The main idea about the use of EnKF is to ensure that the nonlinear unsteady state system is used directly without any form of linearization. Since it is numerical tricky to solve the Saint Venant equation, we consider a scheme based on the finite volume method with staggered grid for obtaining solutions of the unsteady state model in this work. With the staggered grid arrangement, the varying slope of the liquid surface is captured [11]. As the numerical scheme is only suitable for subcritical flow conditions, we consider using a Venturi channel to make the method presented here applicable to supercritical upstream flow condition as well. With this, the method can be applied to non-Newtonian fluid flow where the upstream flow conditions are often supercritical.

In the following sections, the mathematical models describing the system are presented. The algorithm for state estimation of the flow is described. Different results from the algorithm are presented and discussed.

MATHEMATICAL MODEL

The unsteady state flow of fluid in an open channel can be described by the one-dimensional Saint Venant equations [4]:

$$\frac{\partial A}{\partial t} + \frac{\partial Q}{\partial x} = 0 \quad (1)$$

$$\frac{\partial Q}{\partial t} + \frac{\partial\left(\frac{\beta Q^2}{A}\right)}{\partial x} = gA\sin\theta - gA\cos\theta\frac{\partial h}{\partial x} - gAS_f \quad (2)$$

Eq. (1) and (2) are based on mass conservation and momentum conservation principles respectively; Q is the volume flow rate, and A and h are the flow cross sectional area and the free surface level respectively. θ is the angle of inclination of the channel, and g is the acceleration due to gravity. β is the momentum correction coefficient with a value between 1.03 and 1.07. S_f is the frictional slope, and is given by [12,13]:

$$S_f = \frac{n_m V}{{R_h}^{2/3}} \quad (3)$$

where $V = Q/A$ is the average flow velocity, n_m is Manning's roughness coefficient and

$R_h = \frac{A}{P_{wet}}$ is the hydraulic radius at each cross section. In a non-Newtonian fluid flow, the internal frictional shearing stresses dominate; the frictional slope S_f is then given by [12]:

$$S_f = \frac{\tau_y}{\rho g R_h}\left[1 + \left(\frac{(\epsilon+1)(\epsilon+2)|V|}{(0.74+0.656\epsilon)\left(\frac{\tau_y}{K}\right)^{\epsilon} R_h}\right)^{\frac{1}{\epsilon+0.15}}\right] \quad (4)$$

where $\epsilon = \frac{1}{n}$; ρ, τ_y, K and n are the fluid properties denoting the density, yield shear stress, fluid behaviour index and fluid constituency index respectively.

Steady state scheme-ODE form

Considering a rectangular channel: $A = bh$
where $b(x)$ is the width at a given section of the flow, the steady state solution is obtained by solving the following set of ODE's:

$$\frac{dV}{dx} = -\frac{V}{A}\frac{dA}{dx} \quad (5)$$

$$\frac{dA}{dx} = b\frac{dh}{dx} + ch \quad (6)$$

$$\frac{dh}{dx} = \frac{gAS + \beta chV^2}{gA\cos\theta - \beta BV^2} \quad (7)$$

where $c = \frac{db}{dx}$ and $S = \sin\theta - S_f$. From eq. (7), the critical flow occurs when:

$$gA\cos\theta - \beta BV^2 = 0 \quad (8)$$

The depth of the flow which satisfies eq. (8) is the critical depth. The open channel flow is generally characterized by the Froude number, $Fr = \frac{V}{\sqrt{(gh)}}$ [14]. When $Fr < 1$, the flow is subcritical and when $Fr > 1$, the flow is supercritical. The condition is near critical when $Fr \approx 1$.

Unsteady state scheme

Figure 1 shows the grid arrangement. The node of control volume for momentum conservation is indicated by the line **P** where the velocity is stored. The boundaries of the velocity control volume indicated by the lines **w** and **e** correspond to the nodes of the control volumes for mass conservation, where the depths of the liquid surface are stored. The grid is uniform with spatial spacing, Δx. In eq. (2), the spatial integration of the free surface depth gradient is approximated by the central differencing method, and the flux term is approximated by first order upwind [11], and this leads to:

Scheme for volume conservation

$$\frac{dA_i}{dt} = -\frac{Q_{i+1/2} - Q_{i-1/2}}{\Delta x} \quad (9)$$

Scheme for momentum conservation

$$\frac{dQ_{i+1/2}}{dt} = -\beta\frac{(QV)_{i+1} - (QV)_i}{\Delta x} - g\bar{A}_{i+1/2}\cos\theta\frac{h_{i+1} - h_i}{\Delta x} + g\bar{A}_{i+1/2}S_{i+1/2} \quad (10)$$

The boundary discharge, Q_i of each cell can be computed as the average value of the neighboring nodes values. The areas at the nodes $\bar{A}_{i+1/2}$ can be computed with the average depth measured at the boundaries [15].

$$Q_i = \frac{Q_{i+1/2} + Q_{i-1/2}}{2} \quad (11)$$

$$\bar{A}_{i+1/2} = f\left(\frac{h_{i+1} + h_i}{2}\right) \quad (12)$$

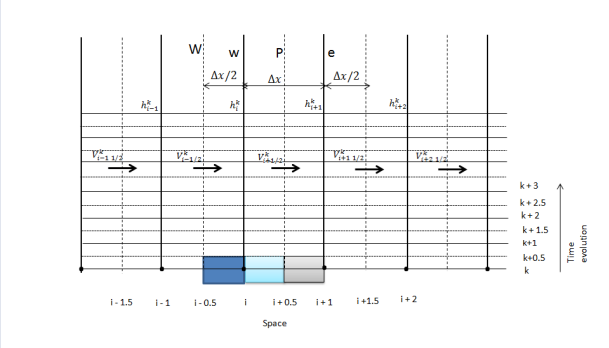

Figure 1: Staggered grid arrangement for V and h control volumes.

Considering only the positive flows, the depths at the boundaries of the mass conservation control

volume and the value of flux, $(QV)_i$ from the momentum equation can be estimated by the following upwind conditions [15, 16]:

$$h_{i+1/2} = h_i \quad (13)$$

$$(QV)_i = \frac{Q_{i+1/2}+Q_{i-1/2}}{2} V_{i-1/2} \quad (14)$$

The stability of the scheme described by eq. (9) through eq. (14) depends on the ODE solver for its implementation. The accuracy is only of first order since the scheme is based on first order upwind conditions.

Boundary conditions

As shown in figure 2, the inlet flow rate Q_{in} is stored at the domain boundary located at $i = 1/2$, and the inlet depth h_{in} is stored at $i = 0$. The outlet values, Q_{out} and h_{out}, are also located accordingly as given in the figure. The values of h at the physical boundaries are obtained by the upwind method, that is $h_{1/2} = h_{in}$ $h_{N+1/2} = h_{out}$ [11]. With $Fr < 1$, both boundaries must be specified (Q_{in} and Q_{out} or h_{in} and h_{out}).

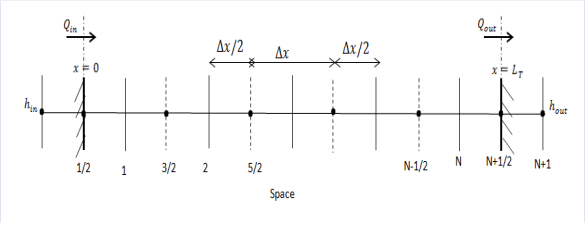

Figure 2: Position of h and Q cells at the domain boundaries.

The solution is based on the so-called backwater curve, implying that the scheme is solved backwards along the domain.

REAL-TIME ESTIMATION ALGORITHM

The algorithm we present here is based on the Ensemble Kalman filter (EnKF) which is based on Monte Carlo simulation of the nonlinear system.

State estimation

Consider a discrete time nonlinear dynamic system given by

$$x_{k+1} = f(x_k, u_k, w_k) \quad (15)$$

$$y_k = g(x_k, u_k, v_k) \quad (16)$$

where x_k and u_k are the state and deterministic input respectively, at time step k, and y_k is the measurement sensor signal at time step k, assumed to be related to system states. $w_k \sim \mathcal{N}(\bar{w}_k, W_k)$ and $v_k \sim \mathcal{N}(\bar{v}_k, V_k)$ are stochastic white noise disturbances in the process and in the measurement respectively at time step k. Both w_k and v_k are assumed normally distributed with respective mean $\bar{w}_k$ and $\bar{v}_k$, and covariance W_k and V_k. The objective is to obtain the estimate, $\hat{x}_k$ of the real state x_k using signal from the level measurement, y_k, so that the covariance $\mathcal{E}[(e_k)(e_k)^T]$ of the estimate is minimized, where $e_k = \hat{x}_k - x_k$, and superscript T implies transposition.

Given the initial condition of the state $x_0 \sim \mathcal{N}(\bar{x}_0, X_0)$, in which $\bar{x}_0$ is the mean value and X_0 is the covariance; assuming there are N_r realizations (ensembles) of x_0 drawn at random such that $x_0^j \sim \mathcal{N}(\bar{x}_0, X_0)$ with $j = 1,2,3,\ldots,N_r$, the forecast of the state estimate and measurement signal for each ensemble point are given by [10]:

$$x_k^{fj} = f\left(x_{k-1}^{aj}, u_{k-1}, w_k^j\right) \quad (17)$$

$$y_k^{fj} = g\left(x_k^{fj}, u_k, v_k^j\right) \quad (18)$$

When the forecasted state estimate, x_k^{fj} for each ensemble point is updated, it gives the analyzed state estimate, x_k^{aj}:

$$x_k^{aj} = x_k^{fj} + K_{xk}(y_k + v_k^j - y_k^{fj}) \quad (19)$$

where v_k^j is a random variable drawn from a normal distribution of data with zero mean and covariance, V_k. K_k is the Kalman gain at time step k, given by:

$$K_{xk} = Z_{xk}E_k^{-1} \quad (20)$$

Z_k and E_k are the cross and innovation covariance matrices respectively given by:

$$Z_{xk} = \frac{1}{N_r-1}\sum_{j=1}^{N_r}(x_k^{fj} - \hat{x}_k^f)(y_k^{fj} - \hat{y}_k^f)^T \quad (21)$$

$$E_k = \frac{1}{N_r-1}\sum_{j=1}^{N_r}(y_k^{fj} - \hat{y}_k^f)(y_k^{fj} - \hat{y}_k^f)^T \quad (22)$$

where $\hat{x}_k^f = \frac{1}{N_r}\sum_{j=1}^{N_r} x_k^{fj}$ and $\hat{y}_k^f = \frac{1}{N_r}\sum_{j=1}^{N_r} y_k^{fj}$.
The best possible estimate given by this algorithm is the ensemble mean $\hat{x}_k$ of the analysed state estimate, with covariance X_k which measures the uncertainty in the estimated state, $\hat{x}_k$:

$$\hat{x}_k = \frac{1}{N_r}\sum_{j=1}^{N_r} x_k^{aj} \quad (23)$$

$$X_k = \frac{1}{N_r-1}\sum_{j=1}^{N_r}(x_k^{aj} - \hat{x}_k)(x_k^{aj} - \hat{x}_k)^T \quad (24)$$

Because the ensemble spread may be too small to draw the model states to the observations [17], a coefficient f_x having value within $0 < f_x < 1$ is introduced to minimize the forecast error variance.

$$K_{xk} = f_x Z_{xk}E_k^{-1} \quad (25)$$

Performance of the estimation

The performance of the algorithm over the computation domain (cells $1 = 1,2,3,\dots,N$) is analyzed based on the relative error given by:

$$e_{rk} = \sqrt{\frac{\sum_{1=1}^{N}(\hat{x}_{i,k} - x_{i,k})^2}{\sum_{i=1}^{N}(x_{i,k})^2}} \quad (26)$$

where $x_{i,k}$ and $\hat{x}_{i,k}$ are the true state and estimated state respectively at cell i and time step k.

Parameter estimation

Effective application of the EnKF algorithm assumes that the system model is perfect. It implies that the algorithm does not account for any deficiency such as model parameter uncertainty. In real-time state estimation, the model time invariant parameters need to be estimated and then augmented into the state vector. As given in [18], the parameter estimation algorithm has the same structure as that of the state.

Let θ be any parameter of the model, and let θ_0 be the measured parameter. Supposing there are N_r realization of θ_0 such that $\theta_0^j \sim \mathcal{N}(\overline{\theta}_0, P_0)$ with $j = 1,2,3,\dots,N_r$, and $\overline{\theta}_0$ and P_0 the mean and covariance of the distribution respectively, the propagation of the parameter in time is given below.

Forecast: $\theta_k^{fj} = \theta_{k-1}^{aj}$ (27)

Corrected: $\theta_k^{aj} = \theta_k^{fj} + K_{\theta k}(y_k + v_k^j - y_k^{fj})$ (28)

where

$$K_{\theta k} = \alpha_\theta Z_{\theta k}E_k^{-1} \quad (29)$$

$$Z_{\theta k} = \frac{1}{N_r-1}\sum_{j=1}^{N_r}(\theta_k^{fj} - \hat{\theta}_k^f)(y_k^{fj} - \hat{y}_k^f)^T \quad (30)$$

and $\hat{\theta}_k^f = \frac{1}{N_r}\sum_{j=1}^{N_r}\theta_k^{fj}$. The ensemble mean of the corrected forecast parameter gives the best possible estimate of the parameter.

$$\hat{\theta}_k = \frac{1}{N_r}\sum_{j=1}^{N_r}\theta_k^{aj} \quad (31)$$

The coefficient $\alpha_\theta > 0$ is used to correct the small spread of the ensemble so that the variance between the estimated parameter and the true value is minimized.

RESULTS AND DISUSSION

The model described by eq. (5), (6) and (7) was used to simulate a fluid flow in a Venturi channel to ascertain the flow conditions. The results obtained by applying the real-time estimation algorithm described in this paper are presented here. All the simulations were done in MATLAB with ode23 for the steady state and ode15s for the unsteady state scheme.

Venturi channel and the Real system

The Venturi channel used in this work is taken from [19]. In this paper, we modified the channel throat width from 0.2m to 0.06m so as to ensure that the supercritical upstream flow jumps to subcritical flow level and then passes through the critical depth at the throat while accelerating towards the channel end.

The "real system" was obtained by simulating the model detailed under the unsteady state scheme section with arbitrary initial conditions. The measurement signal was related to the flow depth taken at the middle of the computation domain with number of cells $N = 50$. The sampling interval for the measurement is 0.25 second. The properties of the real system are given below [20]:
Fluid properties: $\rho = 1034 kg/m^3$, $K = 0.006 Pa.s^n$, $\tau_y = 12.698 Pa$, $n = 1.00$
Channel width: $b = 0.06m$
Channel slope: $\theta = 5\ deg$
Boundary flow rate: $Q = 21.017\ l/s$

The process noise, W and measurement noise, V covariance are each set to $1\text{x}10^{-8}$. The fitted covariance for the estimated states are $5\text{x}10^{-7}$ for the level and $3\text{x}10^{-7}$ for the flow rate. The covariance for the measurement noise in the estimated states was fitted to$1.5\text{x}10^{-4}$.

Steady state flow profile

Figure 3 shows the flow profile of the non-Newtonian fluid (bentonite-based) simulated in the Venturi channel. The upper plot gives the variation of the fluid level, and the lower plot the profile of Froude number associated with the flow along the channel. The figure shows that hydraulic jump occurs at the contraction, transiting the flow from supercritical upstream condition to subcritical condition. It can also be

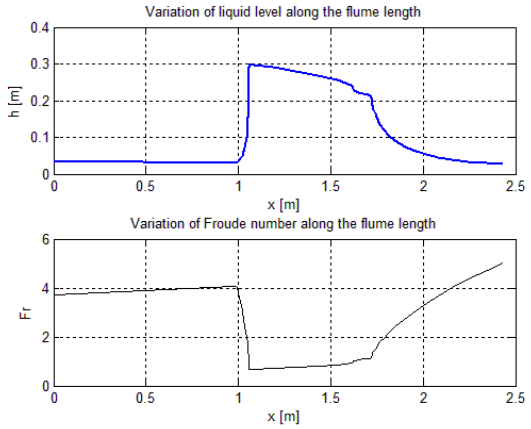

Figure 3: Steady state gradually varied flow profiles with a supercritical upstream flow in a rectangular flume.

seen that the flow passes through a critical depth in the throat where $Fr = 1$. The result shows that measurement of the fluid states (h or Q) can be taken at the throat where $Fr < 1$, and the unsteady state scheme described in this paper can be applied only within the throat section since the numerical scheme only considers subcritical flow conditions.

State estimation

Both the estimated states and model parameter are compared with those of the real system. In all cases, the simulation was carried out for 85 time steps. We also assumed that the boundary conditions of the system are known and fixed.

Ensemble size

Figure 4 shows variation of the mean square error (MSE) of the estimated states at the middle cell (26^{th} cell) over 85 time steps against the ensemble size, N_r with $f_x = 1.0$ (upper plot), and the MSE against the spread coefficient (gain factor), f_x with $N_r = 60$ (lower plot). The result shows that MSE of both flow rate and level decrease as the N_r increases. When $N_r > 50$, it shows that there is no much significant different in the error. With $N_r = 60$, the result shows that MSE of the flow level is minimum at $f_x \approx 0.75$. The MSE of flow rate slightly decreases with decreasing f_x.
In the subsequent results shown in this section, we use the values $N_r = 60$ and $f_x = 0.75$ in the simulations.

Perturbed system with correct model parameters

Figure 5 compares the estimated states with the true states of the system when there is no uncertainty in the model parameters. The upper plots are the flow profiles over the computation domain simulated after 20 seconds ($k = 81$), and the results show that estimation of both the flow rate and the fluid level are good within a tolerable limit. Figure 6 shows the time evolution of the relative error of the estimates for both level (upper plot) and flow rate (lower plot). In both plots, the errors rapidly drop after 2 time steps from the initial value to a value relatively constant over time. It can be seen that the average relative error is about 1.0% for the level and 0.7% for the flow rate. The relative error measures the spread of the estimated states around the real state over all the cells in the domain, and the time evolution shows that the error is approximately the same as the time elapses.

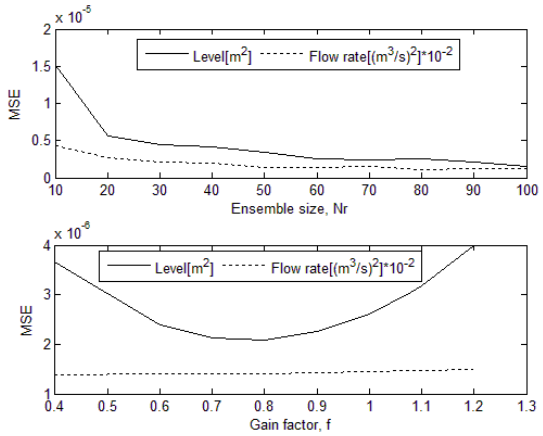

Figure 4: Variation of mean square error at the measured point with ensemble size (upper plot) and with ensemble spread coefficient (lower plot).

System with uncertain model parameters

The results of using uncertain model parameters are presented here. The results compare the estimated states with the true state when the channel width used in the model is 0.059m as against 0.06m used in the real system. Figure 7 (a) shows that the estimated flow level is very poor when the model parameter estimation algorithm is not incorporated in the state estimation algorithm, and the variance in the result is due to uncertainty in the measurement of the channel width. Comparing figure 7 (a) (lower plot) with figure 5(b) (lower plot), it shows that within the width measurement uncertainty the estimated flow rate is not significantly affected; this is also shown by the evolution of the relative error of the flow rate estimate, figure 7(b) (lower plot). The relative error of the estimated level, figure 7(b) relatively increases after time step 2, showing that the estimation yields poor results with time. The uncertainty in the channel width affects the estimation of the flow level possibly because both

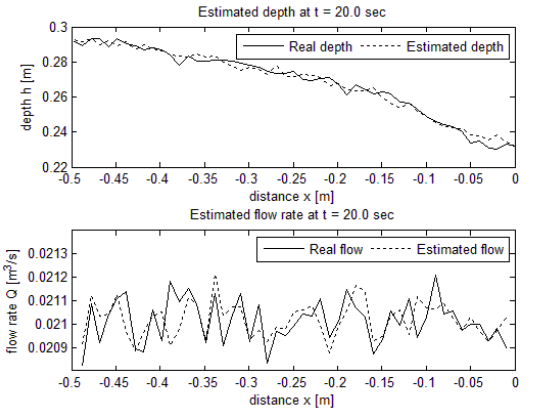

(a)

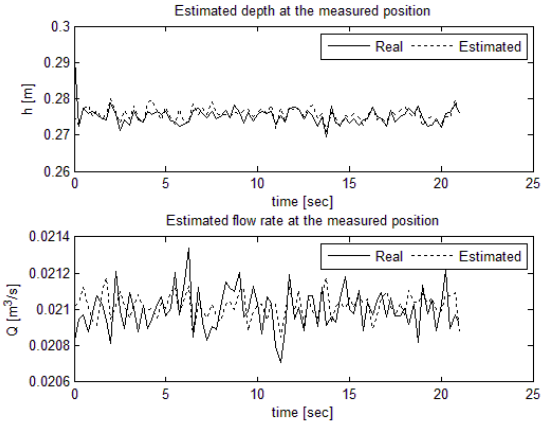

(b)

Figure 5: Comparison of the estimated state with the real state: (a) flow Profile along the domain at time step 81 (b) time evolution of the states at the middle cell.

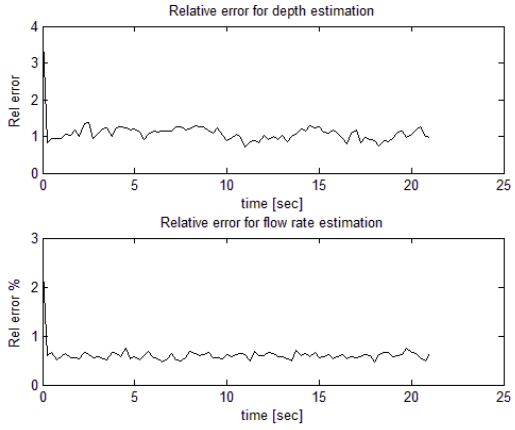

Figure 6: Time evolution of the relative error of the estimated states: flow level (upper plot); flow rate (lower plot).

quantities have the same dimension and because the flow level directly depends on the channel width for a given flow area.

Figure 8 shows the results when the parameter estimation model is incorporated into the state estimation algorithm. Comparing figures 5(b) and 8(a), it shows that the states estimation is relatively the same. Figure 9 shows the evolution of the estimated channel width with time. It can be seen that the width (curve line) rapidly increases reaching the real system width (straight line) after about 7.0 sec. The result shows that after 7.0 sec, the estimated width has a mean value of about 0.06m with mean error of ±0.042% over the simulation time.

CONCLUSION

In this paper we investigated the possibility of estimating the flow rate of a non-Newtonian fluid in an open channel by using the ensemble Kalman filter (EnKF) algorithm. Due to possible uncertainties in the model parameters, we incorporated estimation of the parameters into the state estimation algorithm. Although the numerical scheme for solving the unsteady state of the system considers only subcritical flow conditions, we found that by using a Venturi channel with adequate contraction, the scheme can also be applied to a non-Newtonian fluid flow with supercritical upstream conditions within the throat where the flow is subcritical. The results for assimilating one measurement of the free surface level taken at the middle of the throat into the state forecast showed that the real-time estimation algorithms we presented here are capable of estimating the wavy nature of the states due to process disturbances and measurement noise within $\pm 0.7\%$ accuracy for the flow rate and $\pm 1.0\%$ accuracy for the free surface level. The main challenge in applying the scheme to the flow

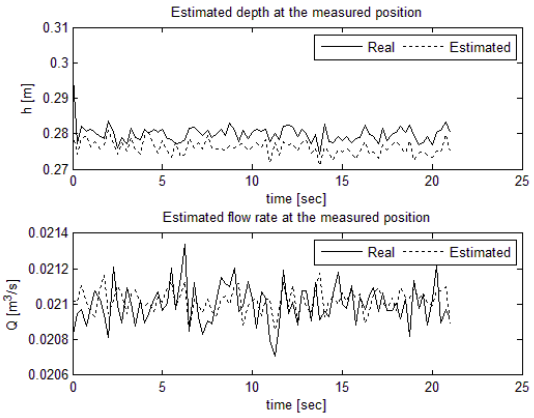

(a)

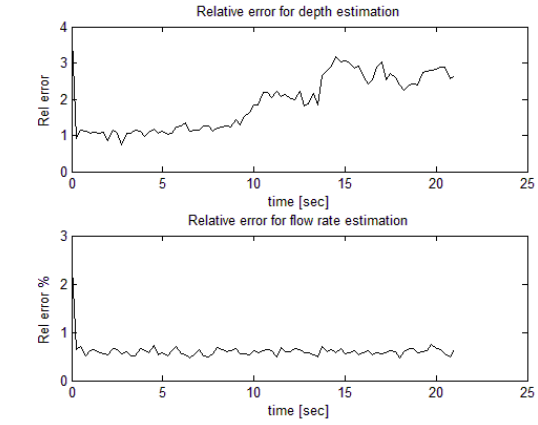

(b)

Figure 7: Comparison of the estimated state (without parameter model) with the real state: (a) time evolution of the states at the middle cell. (b) time evolution of the relative error of the estimated states.

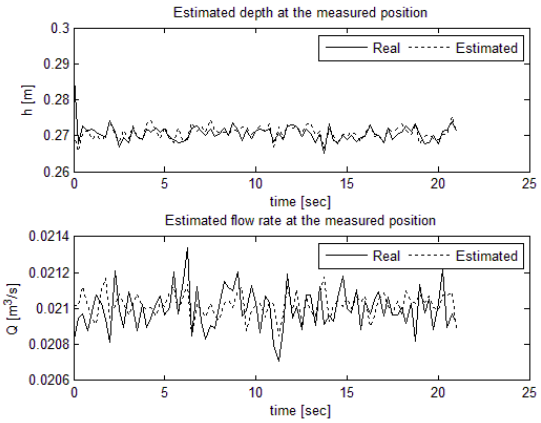

(a)

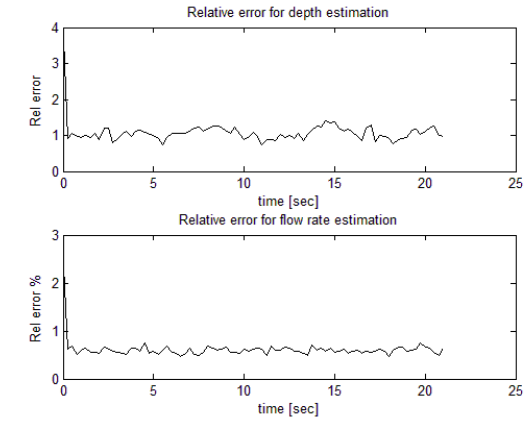

(b)

Figure 8: Comparison of the estimated state (with parameter model) with the real state: (a) time evolution of the states at the middle cell. (b) time evolution of the relative error of the estimated states.

in a Venturi channel is locating the position of the critical depth used as the downstream boundary condition in the throat. Since it is possible that the flow rate at the boundary can change in real time, we will investigate the method for estimating the boundary flow rate and how it can be incorporated into the state estimation algorithm in future work.

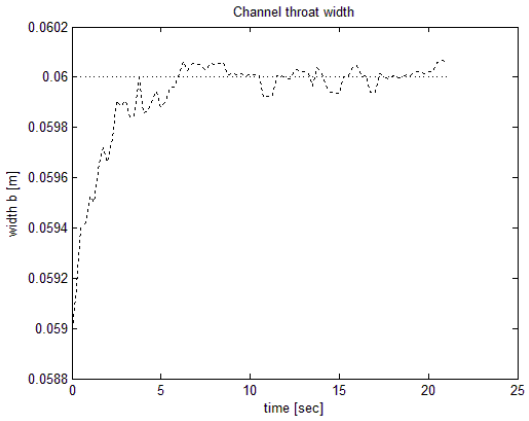

Figure 9: Estimated time-invariant channel width.

ACKNOWLEDGEMENT

The support from Statoil ASA, the Intelligent Drilling group by Bjørn Rudshaug, is gratefully acknowledged.

REFERENCES

[1] Balmforth NJ, Craster RV. *Geophysical aspects of non-Newtonian fluid mechanics*. Geomorphological Fluid Mechanics 2001; LNP 582: 34 - 51.

[2] Ministere du Developpment durable, de L'environment et Desparcs du Que'bec (2007). *Sampling guide for environmental anlysis: booklet 7 - flow measurement methods in open channels*. May 2007, Centre d'expertiseen analyse environmentale du Que'bec, 223p.

[3] Clemens AJ, Wahl, TL, Bos, MG, Replogle JA. *Water measurement with flumes and weirs*, Publication 58. The Netherlands: International Institute for Land Reclamation and Improvement, 2001.

[4] Szymkiewicz R. *Numerical modeling in open channel hydraulics (Vol.83),* Springer, ISBN 978-90-481-3673-5, 2010.

[5] Reddy JM. *Kalman filtering in the control of irrigation canals*. Applied Mathematical Modelling 1995; 19.

[6] Durdu ÖF. *A comparison of recursive least squares estimation and Kalman filtering for flow in open channels*. Turkish Journal of Engineering and Environmental Sciences 2005; 29: 171-183.

[7] Rafiee M, Wu Q, Bayen AM. *Kalman filter based estimation of flow states in open channels using Lagrangian sensing*. In: 48th IEEE Conference on Decision & Control, Shanghai, 2009.

[8] Wu Q, Litrico X, Bayen AM. *Data reconciliation of an open channel flow network using modal decomposition.* Advances in Water Resources 2009; 32: 193-204.

[9] Tossavainen O-P, Percelay J, Tinka A, Wu, Q, Bayen AM. *Ensemble Kalman filter based estimation in 2-D shallow water equations using Lagrangian Sensing and state augmentation*. In: Proceedings of the 47th IEEE Conference on Decision and Control, Cancun, 2008.

[10] Gillijns S, Mendoza OB, Chandrasekar J, De-Moor BLR, Bernstein DS, Ridley A. *What is the ensemble Kalman filter and how well does it work?* In: Proceedings of the 2006 American Control Conference, Minneapolis, 2006.

[11] Versteeg HK, Malalasekera W. *An introduction to computational fluid dynamics: finite volume method*, 2nd ed. England: Pearson Education Limited, Edinburgh Gate Harlow Essex CM20 2JE, 2007.

[12] Jin M, Fread DL. *One-dimensional routing of mud/debris flows using NWS FLDWAV model, in debris-flow hazards mitigation: mechanics, prediction, and assessment*, Edited by Chen-lung Chen, ASCE, New York, 1997: 687-696.

[13] Jeppson R. *Open Channel Flow: Numerical Methods and Computer Applications*. Boca Raton: Taylor and Francis Group, 2011.

[14] Wilson KC. *Flume design for homogeneous slurry flow*. Particulate Science and Technology 1991; 9: 149 – 159.

[15] Aldrighetti E. *Computational hydraulic techniques for the Saint Venant equations in arbitrarily shaped geometry*, PhD thesis. Trento, Italy: Universit`a degli Studi di Trento, 2007.

[16] Stelling GS, Duinmeijer, SPA. *A staggered conservative scheme for every Froude number in rapidly varied shallow water flows*. International Journal for Numerical Methods in Fluids 2003; 43: 1329 - 1354.

[17] Lin C, Wang Z, Zhu J. *An ensemble Kalman filter for severe dust storm data assimilation over China*. Atmospheric Chemistry and Physics 2008; 8: 2975 - 2983.

[18] Yang X, Delsole T. *Using the ensemble Kalman filter to estimate multiplicative model parameters.* The International Meteorological Institute 2009; 61A: 601 – 609.
[19] BAMO Measure. *Flow rate measurement in open channel: DF 2500 Instructions manual*. Argenteuil: BAMO Control Ltd., 2009.
[20] Haldenwang R. *Flow of non-Newtonian Fluids in Open Channels*, PhD thesis. Cape Town, South Africa: Cape Technikon, 2003.